Friction measurements in granular media

Wolfgang Eber
Technische Universität München, Arcisstrasse 21, 80333 München, Germany
(Received 12 June 2003; revised manuscript received 4 November 2003; published 27 February 2004)

We present some experimental results, estimating the lateral stress response to a longitudinal stress applied to an ideal granular system as a function of friction parameters. Structural effects are taken into account through the use of an angle of contact distribution. The two-dimensional model, based on mainly equally sized cylinder granules allows one to derive a dependency of the friction between single granules and the overall angle of friction, which is commonly used to describe the macroscopic behavior of granulate material.

DOI: 10.1103/PhysRevE.69.021303 PACS number(s): 45.70.Qj

I. INTRODUCTION

The behavior of granular material has been studied previously by many scientists [1,2]. In particular, the state of static and slowly sheared systems has been the subject of several investigations [3–13]. The current availability of affordable computing power has given rise to simulations [14,15], since the indefinite position of a single granule within the lot prohibits analytical approaches to detailed characterizations.

However, civil engineers know that granular media behave very well according to phenomenological laws [16–23]. Several attempts have been made to describe them from a more theoretical point of view.

Besides the characterization as a conglomerate, consisting of a large number of granules, where position and orientation of single contacts are not defined, the contact itself is determined only through friction, which introduces another indefinite property of the lot [11,24].

Civil engineers describe granular soil mainly through properties like the angle of friction φ_0 and cohesion c. Previous famous investigators like Coulomb [25,26] and later Rankine [27,28] have built up very basic and well-founded theories on just these characteristics. Some more recent developments can be found in Refs. [16–23,29–33].

Experimental results concerning friction are not easy to obtain in a reproducible manner. Nevertheless, the important role that friction plays within this context motivated us to perform the most basic experiment of soil mechanics: We established an elementary two-dimensional model of granular soil, consisting of well defined granules both in form and parameters of friction, and measured the lateral stress $\sigma_3(\varphi_0)$ in response to longitudinal compression stress σ_1 as a dimensionless averaged factor $\overline{k_s}(\varphi_0)=\sigma_3(\varphi_0)/\sigma_1$.

The experimental setup and the results of these experiments are presented below.

II. EXPERIMENTAL SETUP

Figure 1 shows the experimental setup. A strong aluminum-frame surrounds a vertical experimental volume, which is formed by two parallel plates of glass, set at a distance of 12 mm. This permits good observation from the lateral side, while forces and deformation can be applied from any direction by moving steel boundaries (''walls'') in and out. Forces up to 300 N can be imposed on the equipment without significant strain. The inner surfaces of the ''walls'' are covered with PTFE in order to minimize frictional boundary effects.

A. The granular system

The experimental volume of interest (240 mm×210 mm×12 mm) is filled with small cylinders, made from photoelastic plastics.

The distribution of cylinder diameters was chosen around a nominal value of 10 mm, allowing enough variance to inhibit effects derived from the symmetry. A minimum diameter of 8 mm was selected to avoid clamping, while only a very few cylinders reach a maximum of 30 mm to ensure a sufficient number of contacts within the volume (Fig. 2). A total number of about 400 cylinders in the volume provides an average of 20 contacts to each side wall, contributing to the particular force measurement.

While the cylinder core material is mainly polyester resin, the required variation in angles of friction is achieved by the use of different coatings applied to the circumference.

One set of cylinders was uncoated polyester (PET), a second set was coated with Teflon tape (PTFE), and a third set was enveloped in polyolefin (POC) sheathing. To enlarge the number of available coefficients of friction, a fourth type of cylinder is used, which is completely made of polyvinylchloride (PVC).

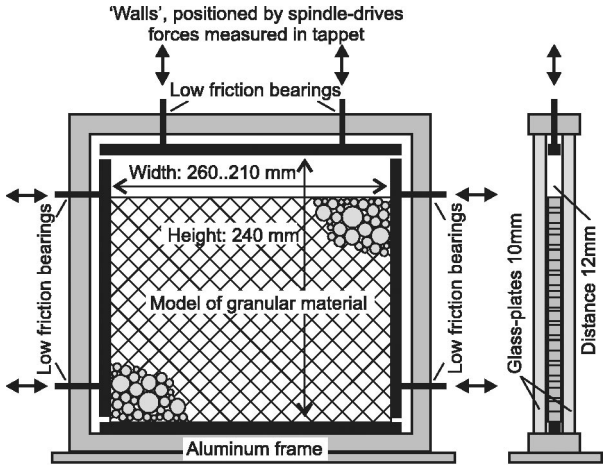

FIG. 1. Schematic view of experimental setup.

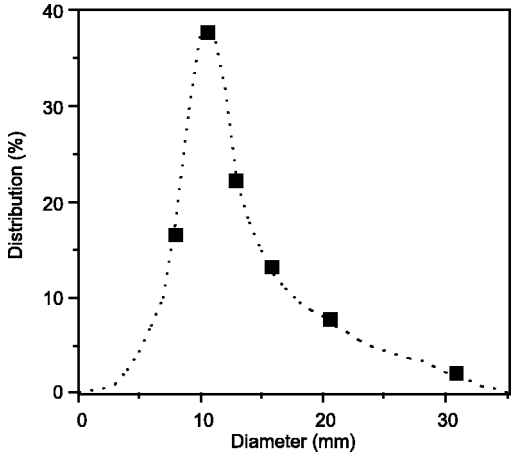

FIG. 2. Distribution of cylinder diameters.

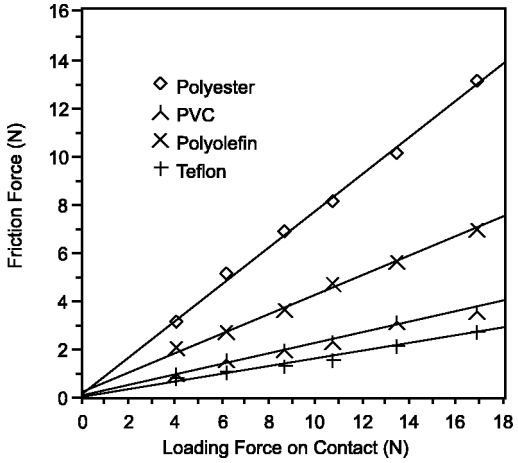

FIG. 3. Friction forces measured on different coatings PET, PVC, POC, and PTFE.

B. The force transmission

The setup allows the application of feeding forces up to 300 N from any side except from below. Electric spindle drives supply active positioning independent of forces, while low friction pneumatic cylinders allow for position-independent constant forces.

All forces are observed by industrial load cells, positioned within the mounting tappets of the movable ''walls.'' In this way, accumulated forces of the total granular volume are measured. The signals were recorded using a locking amplifier, fixed on a 1000 Hz sine wave excitation. Measurements are possible up to 100 Hz for 10 channels with an accuracy of $\approx 0.3\%$.

Positions are read out roughly through potentiometric sensors over a range of 100 mm ($\pm 0.1\%$), where small variations are observed using dial gauges (accuracy ± 0.01 mm).

Data acquisition is run through a PC-based data logger, to be recorded, interpreted and stored.

III. FRICTION MEASUREMENTS

Besides the structural impact on the behavior of granular material, the coefficient of friction μ_0 can be taken to be the most important parameter.

While the common approach [16,17,25–27] defines the coefficient of friction inversely from the response of the granular system as an effective parameter, the influences of structure and friction need to be separated. Therefore, the microscopic coefficient of friction was measured carefully in advance in order to correlate it to the observed behavior.

Efforts have been spent on understanding microscopic frictional mechanisms by a number of researchers [34,35]. Currently a continuous transition from static to dynamic friction is established based on a strong dependency on the velocity of a contact. In particular, *velocity weakening* causes the coefficient of friction to increase significantly with decreasing contact velocity in the range of 10^{-1} mm/s to 10^{-4} mm/s. Thus, μ_0 can rather not be treated as a constant but needs to be corrected by a logarithmic function of the displacement speed. Measuring μ_0 at the state of incident failure would provide a correct static value, yet it still depends on the age of the contacts. This introduces some difficulty in choosing a proper method to obtain representative friction coefficient values μ_0.

Since this work aims at the structural impact on effective friction, we decided to measure the coefficients under circumstances as close as possible to the conditions found in the granular system. As the granulate material is sheared slowly by a spindle drive (see Sec. V A), lost contacts are constantly replaced by new contacts. Hence, we used the same model at the same velocity to obtain representative friction coefficients: A slowly moving contact is repeatedly opened and closed while the varying friction force is observed. We suppose in particular, that the rise of the retaining force when closing the contact represents the situation best and yields proper coefficients of friction for comparison purposes with the behavior of complex granulate material.

To implement such an experiment, a single contact of the particles involved was loaded with different forces and then moved slowly for a distance of some 10 mm in order to eliminate local irregularities. The measurement is then repeated moving in the opposite direction, averaging mechanical effects.

Conventional load cells are used in conjunction with a sensitive locking amplifier to record the retaining friction force. The different loads are gauged using the same system prior to the actual measurement.

The speed of moving was set to about 0.25 mm/s, using the same electric motor spindle drive which imposes the shearing displacement in the next sections measurement.

While moving, the load was repeatedly removed and reapplied. These reapplied load steps can be observed well, even on widely varying underground, and allow for regressional analysis to determine the ratio μ_0 of the friction force F_R to the normal force F_N (see Fig. 3).

The tested surface materials were Teflon (PTFE), polyvinylchloride (PVC), polyolefin (POC), and polyester (PET). In order to verify the reproducibility, some of the measurements were repeated with positively validating results.

Mean values, taken from one load, together with the load itself, were plotted on graphs. Then regression lines were computed to represent the gradient $\overline{\mu_0}$. Since the interpolation lines meet the origin of the graph within their error

TABLE I. Measured coefficients of friction for different coatings.

Material	Teflon	PVC	Polyolefin	Polyester
R^2 (means)	0.975	0.990	0.997	0.996
Gradient $\overline{\mu_0}$	0.136	0.200	0.358	0.736
Accuracy (95%) (+/−)	0.016	0.028	0.028	0.052
Corresp. angle of friction arctan $\overline{\mu_0}$	7.75 deg	11.33 deg	19.71 deg	36.34 deg
Interval of confidence (95%) (deg)	+/−0.86	+/−1.56	+/−1.60	+/−2.99

margins, cohesion $c \simeq 0$ is obtained as expected for dry friction.

Fairly high coefficients of regression R^2 allow for a first order approximation of the result, neglecting nonlinear influences of the hertzian nature of the contacts. In order to obtain a reasonable error estimation, all results concerning a combination of materials were taken into account for further regression analysis.

As was expected, the single values show a wide variation due to the statistical nature of the contacts. Nevertheless, regression analysis of the measurement, taking into account about 150–200 ''steps'' per combination of materials yields amazingly good and reproducible results (see Table I).

Remark. The angle $\vartheta_0 = \arctan \overline{\mu_0}$ is a microscopic parameter and therefore not equivalent to the angle of friction φ_0, which is defined by the macroscopic behavior of the material. Here it is specified only for clearness. In the following, $\overline{\mu_0}$ respectively $\vartheta_0 = \arctan \overline{\mu_0}$ is always used for the microscopic friction, while φ_0 represents the macroscopic angle of friction.

IV. ESTIMATION OF UNEVENNESS

Due to the fabrication process, the cast cylinders display significant unevenness. Assuming constant distribution of contacts over the whole range of angles, this property might be ignored, since such irregularities provide symmetrically rising and falling slopes, where additional positive and negative terms to the angle of friction cancel each other. Yet on the basis of self-organizing processes this symmetry cannot always be preconditioned.

In order to understand the circumstances of our measurements, the unevenness was recorded. While turning a cylinder between two sensing heads, the absolute height of irregularities for every type of surface material were surveyed and mapped (see Table II).

The statistical errors are high due to the random selection of tested cylinders. Nevertheless, the amount of noise read from the smooth PVC cylinders produced on the lathe serves as a well defined indication for the quality of the measurements. Thus, the error can be assumed to be about 21%.

TABLE II. Unevenness of cylinders due to the casting process.

	Polyester	Polyolefin	PVC	Teflon
Mean roughness (mm)	0.24	0.23	assumed even	0.23
Error (95%) (mm)	0.07	0.09		0.11

V. COEFFICIENT OF LATERAL STRESS

Most of our work aims at the measurement of the lateral stress σ_3, responding to longitudinal stress σ_1, applied to a model of granulate material with a well defined coefficient of friction in comparison to approved theories like that of Rankine [27,28]. In contrast to his approach, we are observing not a complete ''soil'' situation but a volume, small enough to be independent of boundary conditions, but still large enough that discreteness of the grains has no more influence. In all measurement assemblies, the horizontal axis is the x axis, positive to the right, while the vertical axis is the y axis, positive to the top. Pressure is always taken to be positive while drag is negative.

A. Constructing an unambiguous state

Due to the nonlinear character of friction playing the dominant roll in granular systems, a grain contact can bear a wide range of tangential forces without making this visible to an external observer. Thus, only the boundary states, where friction helps most to withstand a deformation can be observed and are of greater interest. These two available border states, in both positive and negative directions are closely related to the ''active'' and the ''passive'' state defined by Rankine, and therefore denoted accordingly in this paper. Since the states are symmetrical, it is sufficient to survey one of these. We define it by compressing a granulate volume in the horizontal direction, where friction between the grains inhibits deformation. With increasing stress, deformation takes place because friction forces are now not strong enough to prevent movement. Vertical expansion is then observed, the stress no longer increases and the border state is reached.

However, well determined measurements presuming this state all over the volume can only be achieved by carefully creating the motion history of the model. Due to the stochastic character of the building of structures, many motion cycles described above had to be executed and analyzed in order to obtain reproducible results.

All measurement cycles have been taken in the same manner (see Fig. 4): Into a fixed two-dimensional volume, containing the granulate, the left wall is pushed inwards, forcing the granules to rise to the top [Fig. 4(a)]. Besides the small friction force introduced by the experimental apparatus, an additional basic force is needed to shear the system against its own weight. Then, with a little more pressure, the

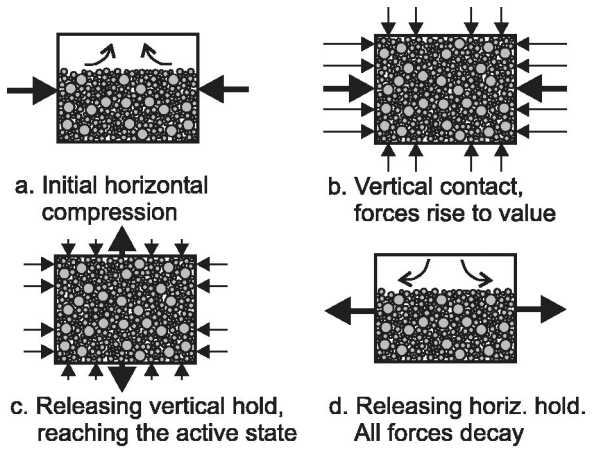

FIG. 4. Measurement cycle to achieve the active state. Bold arrows indicate motion; light arrows are forces.

desired horizontal force is applied to the granulate [Fig. 4(b)].

Holding this for a while, a bit of creeping is observed, when single contacts are shifting to reach more stable positions. This behavior tends to move the system away from the border state. Therefore, the upper wall of the volume is slowly lifted by about 300 μm to allow the system to reach it definitively [Fig. 4(c)]. In this way, the vertical as well as the horizontal forces decrease slightly. At the end of this process to ensure the limiting state, the granulate immediately begins to lose this state again, proven by a small rise of the vertical force while horizontal forces are still decreasing.

Finally, the left wall is driven back to its initial state, where all the forces are expected to vanish and the setup is ready for another cycle [Fig. 4(d)].

The characteristic stress development of such a cycle is shown in Fig. 5. Several aspects had to be considered carefully, to achieve a satisfactory interpretation of the factor $\overline{k_s}(\varphi_0)=\sigma_3(\varphi_0)/\sigma_1$ in the desired border state.

Calibration of the load cells has to be made before and after every set of measurements.

The more or less constant friction forces of the setup must be eliminated.

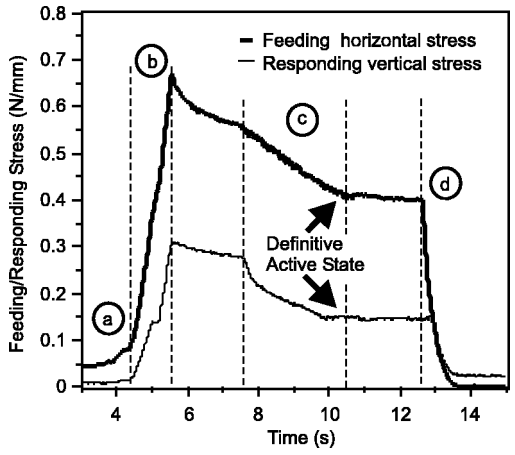

FIG. 5. Stress development during a typical cycle.

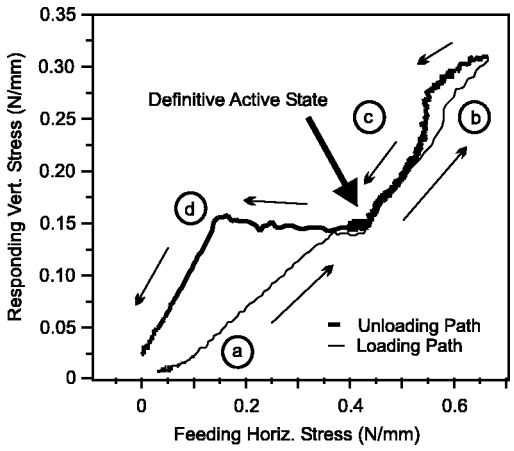

FIG. 6. Typical cycle; hysteresis diagram.

Care must be taken to certainly localize the final active state of the granulate material. Further tests have been performed successfully in order to gain certainty of this state.

Because of the stochastic character of the problem, only mean values can be obtained. Their variance does not tell much about the quality of the measurement, but indicates the broadness of responses to the possible states. Thus, many samples will indicate only the distribution of arrangements and will certainly not sharpen the distribution around the mean value.

In order to interpret the cycles, the force transmission was displayed against the force response to obtain significant hysteresis diagrams (Fig. 6).

In preparation of the workout, the hysteresis diagrams of all cycles were analyzed with the following results.

In general, the properties, mentioned above, can easily be observed. Especially the point where the granulate material is completely activated is well defined. Besides the fact that this point can be just ''seen,'' it is bound to be the minimum gradient, observed within the cycle. Any other higher gradient will not denote the active state.

On the basis of this, several cycles have been carried out with different maximum horizontal forces. Thus, each of the well-defined ''active'' points of every cycle lies on a different force level. With a proper reference, eliminating friction and systematic errors, the entirety of cycles yields a coverage of the force range that can be analyzed with good results.

The frictional contribution of the experimental setup is very obvious and can be taken into account: After every cycle the horizontal value is somewhat higher, i.e., on expanding the volume. On changing direction and before the granulate starts to be sheared, the horizontal force is observed to be reduced. These constant values will have no effect on the calculation of the gradient.

All changes taking place during the measurement cycle are accomplished after the feeding force has been released. Thus the final state is the best reference for the last cycle.

B. Measuring the lateral stress factors

We expected to observe effects of different character, when the granulate material is compressed horizontally,

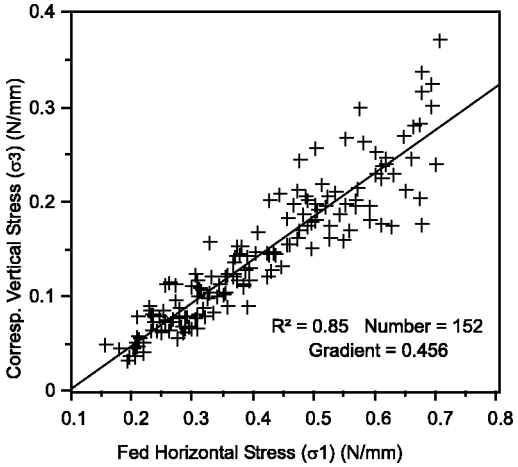

FIG. 7. Subsumption LLO readings; material: PVC.

while it expands freely in the vertical direction. This procedure is likely to allow self organising mechanisms to develop, which cause significant differences in $\overline{k_s}$. On the other hand, the same may lead to relaxation processes, provoking compensation by statistical averaging. Since the process of developing such behavior corresponds to raising the level of organization by forced deformation, in this paper, measurements are classified as being of ''high'' or ''low'' level of organization (HLO or LLO).

To understand these effects and possibly eliminate them, two types of cycles were performed.

For measurements with *low level of organization* (LLO), the volume is filled with carefully mixed cylinders. The size of the window had previously been preset, so that it can be completely filled. After that, the loading branch is characterized by a very small percentage of horizontal compressing before the top is reached and forces begin to rise. The typical horizontal deformation in this process is approximately 5% of the window size.

Expecting strong influences of the initial configuration, for each material thirty sequences were recorded, containing each at least five to six cycles. After every two sequences the granulate material was remixed again to avoid building structures within the system. To be certain of the drift behavior, horizontal as well as vertical gauging was analyzed before and after every ten sequences. Thus, about 170 cycles were provided for further investigation for each of the four surface materials.

Measurements with *high level of organization* (HLO) are characterized by free horizontal deformation of about 20% of the length, before the granules touch the upper bound and the forces begin to rise. Three sets consisting of sixteen sequences were executed. Anticipating balancing effects through the long consolidating range, mixing and reloading the granules was done every two sequences. A sequence contains only two cycles, so overall this yields about 90 pairs of values for each surface material. Gauging again was done before and after each set to keep control over possible drifting effects.

Typical summaries of such a set of values are shown in Fig. 7.

TABLE III. Measured lateral stress factors.

Material	Teflon	PVC	Polyolefin	Polyester
$\vartheta_0 = \arctan \mu_0$(deg)	7.75	11.33	19.71	36.60
Error (+/−) (deg)	0.86	1.56	1.60	2.99
$\overline{k_a^{total}}$(LLO)	0.344	0.456	0.272	0.200
Error 95% (+/−)	0.025	0.031	0.031	0.024
$\overline{k_a^{total}}$(HLO)	0.491	0.452	0.351	0.198
Error 95% (+/−)	0.04	0.03	0.04	0.03
Elastic contrib.	−0.037	−0.037	−0.037	−0.037
$\overline{k_a^{frict}}$(LLO)	0.307	0.419	0.235	0.163
$\overline{k_a^{frict}}$(HLO)	0.454	0.415	0.314	0.161

Depending on influences like creeping values, time dependent effects and low values, some of the measurements are spread wider than others. Regression analysis was used, to eliminate this as well as to give a good estimation for errors. Again, larger deviation from the mean, results from the stochastic character of the generating of structures.

In order to achieve a measure for the plastic behavior introduced by sliding contacts, the elastic contribution as well as the influence of other potential side effects needed to be separated. Investigating this leads to a constant elastic offset $\overline{k_{smean}^{elast}} \simeq -0.037$, while effects from friction to the glass walls came to be less than 0.1% of the initiating load. Friction to the limiting sidewalls turned out to be negligible.

C. Final readings

Finally the results $\overline{k_s}$ of all the sequences are summarized in Table III. Now that they are definitely taken in an active state of the granular material, they can be called $\overline{k_a}$, in accordance with soil mechanics practice.

In this table $\vartheta_0 = \arctan \mu_0$ is the microscopic angle calculated from the coefficient of friction μ_0, where the macroscopic angle of friction φ_0 is assumed to be a function of μ_0. LLO lists the lateral stress factors for *states of low level of organization* (i.e., $\varepsilon \simeq 5\%$) and HLO is the same for granular material with *high level of organization* ($\varepsilon \simeq 20\%$). Error bars are calculated for the 95th percentile. Elastic impact is eliminated from the final result.

The graphs in Fig. 8 and Fig. 9 display the resulting $\overline{k_a^{frict}}$ vs the microscopic angle of friction $\vartheta_0 = \arctan \mu_0$. In order to illuminate the deviation, a theoretical line $k_a^R = \tan^2(\pi/4 - \varphi_0/2)$ in the style of a Rankine approach is added, where equivalence of the microscopic angle of friction ϑ_0 and the macroscopic angle of friction φ_0 is assumed.

VI. DISCUSSION OF RESULTS

The first impression of the observed values is that completely different mechanisms are working on higher deformation (~20%) than on low deformation (~5%).

Starting from a more or less statistical state and allowing no restructuring, some force chains take over most of the longitudinal stress and therefore do not produce much lateral stress. Building up these force chains underlies mainly local

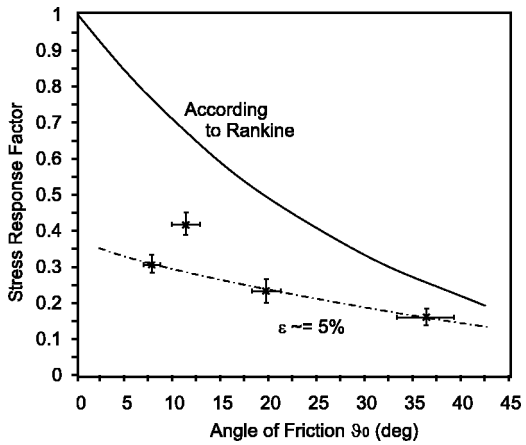

FIG. 8. Measured lateral stress response (LLO).

self-organizing effects, no relaxation processes are available to compensate. Nevertheless, the measurements exhibit a tendency to a smooth line, a good deal beyond the Rankine relation, with an exception of the PVC-material value. This material obviously indicates an additional different effect.

Allowing for further relaxation, under deformation of some 20%, this discrepancy has completely vanished. Additional recorded polariscope images of the granulate, displaying the distribution of stress, show well distributed patterns, with no observable difference between the miscellaneous surface materials. Thus, we assume, that such a forced deformation enables relaxation processes to accomplish and, hence, can serve as a proper model for granulate materials with a known history of unidirectional motion. As long as the motion is much shorter (5–10%) or more random, the predictions become less reliable.

A. Results regarding granulate with high level of organization

Assuming the highly organized state as the model for granulate material not too far away from equilibrium, it needs to be compared to the concept of Rankine.

The basic idea of Rankine was to evaluate a macroscopic coefficient of friction μ_0^{eff} from the ratio of the tangential shearing stress σ^T and the normal stress σ^N in the sliding

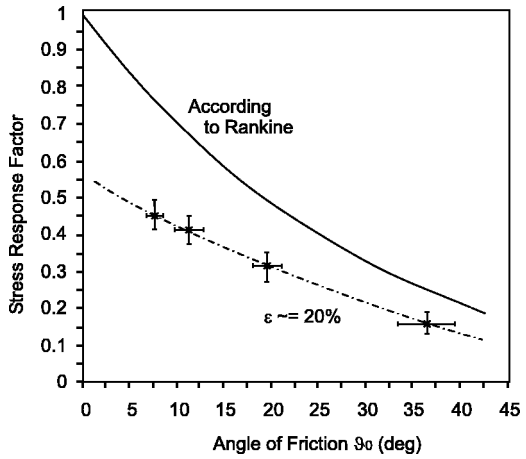

FIG. 9. Measured lateral stress response (HLO).

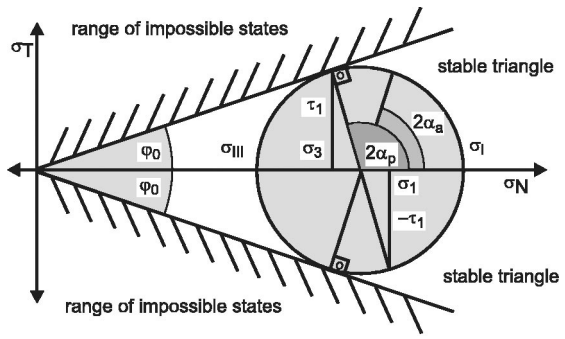

FIG. 10. Stress states according to Rankine.

joint since experiments yielded the state of failure as $\sigma^T/\sigma^N=\mu_0^{\text{eff}}=\tan\varphi_0$ (as far as cohesion c can be assumed $c=0$). This defines the yield surface as a triangle, symmetrically to the stress axis. Any state, defined by the principal stresses (σ_I,σ_{III}) can be transformed in other coordinates and thus shows up as a circle in this space. If this circle touches the limiting triangle the state of failure is reached. The sliding plane is defined by the angle α, by which the system needs to be turned to touch the limiting line. (See Fig. 10.)

According to the limiting characteristic of a frictional force, two limits depending on the direction of movement can be observed, here called the active state and the passive state. The lateral stress factor for the active state is derived as

$$k_a=\tan^2\alpha_a=\tan^2\left(\frac{\pi}{4}-\frac{\varphi_0}{2}\right),$$

where

$$\varphi_0=\arctan\mu_0^{\text{eff}}.$$

The active state is defined, where the lateral wall is yielding and friction is helping to hold the state. Thus $k_a=\sigma_3/\sigma_1$ is less than unity, because σ_3 is reduced by friction. In the passive state the lateral wall tries to move inward and is held stable by σ_1. In this case friction reduces σ_1 which leads to k_p greater than unit. According to the drawing above k_p is determined to be the reciprocal value of k_a.

The measurements shown above display a significant difference to the Rankine equilibrium state, which can be interpreted as the structural contribution in two dimensions.

The shearing process in the sliding joint of a granular material is based on many contacts at varying angles γ within a limit $[-\delta,\delta]$. This is given by the shape of the cylinders as well as the self-organizing process, which is assumed to smoothen the joint, forcing the bedding cylinders in a more or less perfect line.

Therefore, the microscopic coefficient of friction μ_0 is different from the effective operating coefficient of friction μ_0^{eff} (see Fig. 11, clockwise oriented angles are positive).

The local coefficient of friction $\mu_0=\tan\vartheta_0$ in dependence of a contact angle γ can easily be calculated as

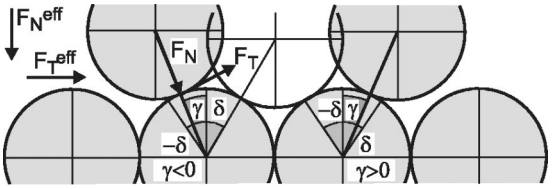

FIG. 11. Geometrical situation in the sliding joint.

$$\mu_0 = \frac{F_T}{F_N} = \frac{F_T^{\mathrm{eff}} \cos\gamma + F_N^{\mathrm{eff}} \sin\gamma}{F_N^{\mathrm{eff}} \cos\gamma - F_T^{\mathrm{eff}} \sin\gamma}.$$

Describing the scene in the sliding joint by the macroscopic angle of friction

$$\varphi_0 = \arctan \mu_0^{\mathrm{eff}} = \arctan \frac{F_T^{\mathrm{eff}}}{F_N^{\mathrm{eff}}},$$

we write

$$\tan\varphi_0 = \frac{\tan\vartheta_0 - \tan\gamma}{1 + \tan\vartheta_0 \tan\gamma} = \tan(\vartheta_0 - \gamma),$$

which identifies $\varphi_0 = \vartheta_0 - \gamma$. Hence, a negative angle of contact γ virtually enlarges ϑ_0.

In order to obtain the mean value, the range for γ to vary needs to be defined. As the drawing (Fig. 11) indicates, the geometrically possible location is limited by an angle $\pm\delta$, given by the straightness of the bedding layer. For perfectly straight lines we have $\delta = 30°$; under less ideal circumstances it might be a bit more.

The equation above additionally yields a natural limit, for φ_0 must not be negative. Thus, we obtain $\gamma \leqslant \vartheta_0$ and therefore $\gamma \in [-\delta, \vartheta_0]$.

Sufficient forced deformation of the granular material as considered here, causes self-organizing processes establishing shear zones, where the granules are *shifted collectively*. Since the collective remains compound, each of the single contacts is not governed by local criteria of friction and movement, but can be assumed evenly spread over all possible conditions. Therefore, the measured unevenness of the cylinders produces as many rising edges as falling edges, where none of these preferably influences the characteristics of a mean contact. This turns out to be a very important observation.

Assuming *constant probability* $P_\gamma d\gamma = d\gamma/(\delta + \vartheta_0)$ within this range, the effective coefficient of friction can be gained through

$$\overline{\tan\varphi_0} = \overline{\mu_0^{\mathrm{eff}}} = \frac{\int_{-\delta}^{\vartheta_0} \tan(\vartheta_0 - \gamma) d\gamma}{\delta + \vartheta_0} = -\frac{\ln[\cos(\delta + \vartheta_0)]}{(\delta + \vartheta_0)}.$$

Applied to the measurement, φ_0 is calculated from ϑ_0 and under assumed evenness of sliding joints, the results fit the theoretical considerations very well. Best fit is gained under the assumption of $\delta = 37.0°$ with a mean deviation of 1.35°.

It should be kept in mind, that this value is a mere fit, but it appears to be very plausible, knowing that a perfectly smooth joint is characterized by $\delta = 30°$. Completely rough joint surfaces would be the normal on stochastic mixtures, far away from equilibrium, which occur on states with low levels of organization.

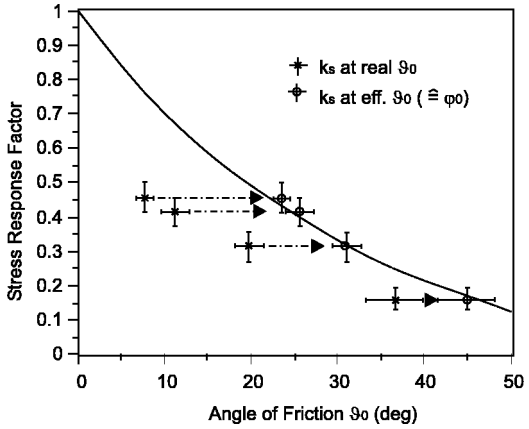

FIG. 12. Measured lateral stress response (HLO) shifted to effective angle of friction.

Improvement might be expected from specifying the *probability of contact proportional to* $\cos\gamma$, keeping in mind the projection of the surface to the slide joint as the relevant face.

Under this condition we have

$$\overline{\tan\varphi_0} = \overline{\mu_0^{\mathrm{eff}}} = \frac{1}{\sin\delta + \sin\vartheta_0} \int_{-\delta}^{\vartheta_0} \tan(\vartheta_0 - \gamma)\cos\gamma d\gamma,$$

which can also be solved fundamentally and gives an effective angle of friction φ_0, which is slightly ($\approx 0.5°$) lower than the one given by a constant distribution of probability. As before, the measurement results can be approximated on the basis of $\delta = 38.1°$, resulting in a mean deviation of 1.12°. The arising effective angle of friction is less than 1% away from the one obtained by the linear approach.

The graph in Fig. 12 shows the structural adjustment to the measurements on highly organized granulate material using the COS distribution. Hence, taking into account angle of contacts distribution leads to a friction dependent correction to the Rankine approach which is compatible with the experimental results.

Remark. Further estimation of self-organizing effects leads to an even better quantitative verification of this result using compensation of the local effects after a continuous deformation of $\varepsilon \simeq 20\%$.

In order to gain an appropriate picture of the situation, we additionally need to consider the *packing fraction* ϱ of the granular system. The values were calculated from the final size of the experimental volume for some different cylinder types in the HLO state and are listed in Table IV.

As these values can be compared to a rough estimation for packing fractions following from the width of the contact angle distributions, they improve the plausibility of the approach made here.

According to Gervois and Bideau [36], who investigated the geometrical properties of monosized 2D hard disk pack-

TABLE IV. Measured packing fraction (HLO).

Material	Teflon	Polyolefin	Polyester
Packing fraction ϱ	0.743	0.728	0.668
Interval of confidence (95%)	$+/-0.031$	$+/-0.037$	$+/-0.019$

ings using Voronoi tessellation, the deviation from a well ordered hexagonal assembly can be expressed as a function of the packing fraction ϱ. The angle α between two adjacent neighbors with respect to the center grain is determined by a distribution characterized by the width $(\Delta\alpha/\alpha_m)(\varrho)$ and the center value $\alpha_m = 60°$.

Based on this dependency, we converted the measured packing fraction ϱ to the corresponding distribution width $\Delta\alpha$ (see Table V).

Considering the model in Fig. 11, the straight bedding layer represents the ideal direction, achieved by a perfectly ordered system. The mean deviation from this state is determined by the width of the angular distribution.

Under the assumption of a simplified constant angular distribution, enlarging δ from $\delta = 30°$ to the obtained optimal value of $\delta \simeq 38.1°$ requires a variation of the contact angles within the bedding layer of $\pm 2 \times 8.1^{\pm 1.1°} = \pm 16.2^{\pm 2.1°}$.

Hence, within the natural limits of such a rough estimation on the basis of monodisperse cylinders, this value corresponds accordingly to the distribution widths obtained from the packing fraction of the granular systems in our experiment.

B. Results regarding granulate with low level of organization

To gain certainty about the characteristics, the results on scarcely organized granulate were repeatedly confirmed by additional series of measurements. They are reproducible and display the shown properties.

The most remarkable attribute is the nonmonotonous progression of the lateral force with the rising coefficient of friction. Especially the value obtained from the PVC material presents itself as a strong misfit.

Even under the assumption that this value is the result of a systematic error, which is not very likely, the remaining data cannot be fitted like the highly organized sequences. Furthermore allowing not much compensating, the approach of Rankine is not directly applicable here.

On the basis of stochastic positioning of the cylinders, angles δ up to 60° occur, so sliding joints cannot really be established. This state is much closer to a statistical model,

TABLE V. Width of angular distribution derived from measured packing fraction (HLO systems).

Material	Teflon	Polyolefin	Polyester
Width of angular distribution $\Delta\alpha$ (deg)	13.56	13.80	15.36
Interval of confidence (95%) (deg)	$+/-0.66$	$+/-0.90$	$+/-0.42$

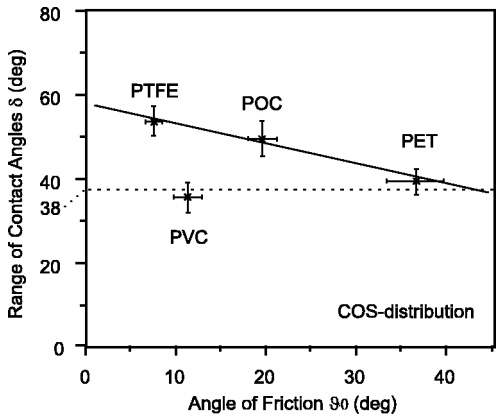

FIG. 13. Extended width of distribution δ derived from LLO measurements.

telling something about the building of force chains bearing most of the load.

Since the readings are much lower than predicted by a quasi continuous model, and as the polariscope images indicate, such a perception is very likely to hold. Unfortunately there is no way to perform the experiments completely without any deformation and thus organization, so mixtures of states as well as effects triggered by small self-organization rates contaminate the results.

Obviously the granular system is observed in the middle of the compaction process where the distribution of contact angles grows narrower depending on parameters of friction.

Attempting to apply the analysis used for the HLO measurements results in values of δ shown in Fig. 13.

Coherently, the range of possible contact angles $[-\delta,\delta]$ is much wider for the investigated systems and reaches up to 54°. Yet, this effect decreases with increasing angle of friction and is not applicable to the PVC coated granulate.

The only property where the PVC cylinders differ from the others is the observed unevenness of the circumference surface. Being produced on the lathe they are perfectly smooth, while all other cylinders had been cast and show small, sharp irregularities.

So, contrary to the arguments discussed before on the highly organized systems, here the local unevenness of the cylinders seems to play a most important role.

The discontinuity displayed by the measurements concerning PVC and teflon cylinders is obviously not supported by any physical argument. There is no reason why the relation between the angle of friction and the produced transversal force should not be monotonous but exhibit a sharp maximum at any value.

Remark. Nonlinear equations ruling chaotic systems are nevertheless likely to produce similar characteristics. Such approaches were applied to comparable systems and promise a good understanding. Yet, motivated by the good reproducibility of the results under varying circumstances, we deduce this not to be the source of the peak.

More probably, small irregularities on the circumference impede the ability of the granular material to compact itself when shearing at low amplitudes. This obviously leads to well compacted PVC cylinders after deformation of $\varepsilon \simeq 5\%$,

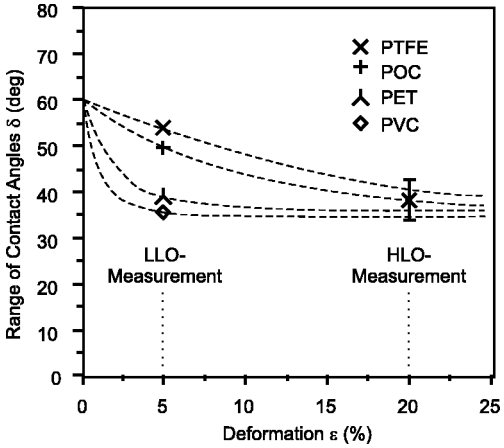

FIG. 14. Qualitatively outlined compaction progress.

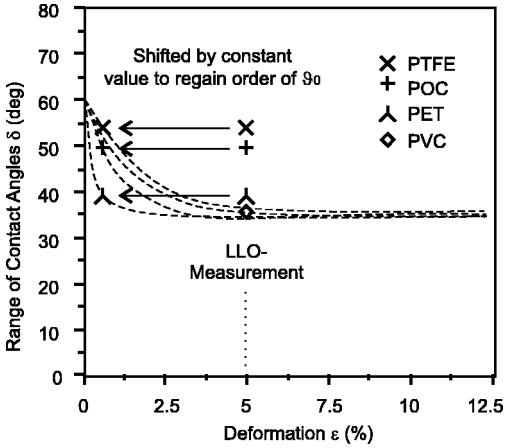

FIG. 15. Compaction progress, corrected for the influence of surface roughness.

while other types of cylinders are not yet compacted at this low shearing amplitude.

In Fig. 14, the compaction process is outlined as the distribution of the angles of contact δ becomes narrower with increasing shearing amplitudes. At $\varepsilon \simeq 20\%$ the state of equilibrium seems to be reached where the microscopic angle of friction as well as the local roughness of the surfaces have no significant impact as they have on the progress of compaction observed at $\varepsilon \simeq 5\%$.

In order to estimate the influence of local roughness on the compaction process, we investigated the local height of the surface irregularities for the coatings used (see Table II).

All cast cylinders exhibit about the same relative surface roughness of $\simeq 4.6\%$, while the cylinders, produced from PVC on the lathe are significantly better and serve as an absolute reference for measurement noise.

The high statistical errors of the measurement data do not allow for quantitative analysis, yet the equal mean values indicate at least comparable influence of the local roughness for the coatings PET, POC, and PTFE in contrast to PVC.

Therefore, assuming an equal magnitude of retarding the compaction, we need to shift the measured values for LLO systems regarding PET, POC, and PTFE by a constant value to still lower shearing amplitudes until the unimpaired PVC measurement fits into the sequence given by the angles of friction (Fig. 15).

This qualitative correction clarifies, that even with shearing amplitudes of $\varepsilon \simeq 5\%$ the compaction process reaches the equilibrium state at $\delta \simeq 38°$, if not local roughness had slowed down the progress.

C. Fitting the measurement results

Finally the HLO and the LLO measurements lead to the same result $\overline{k_a}(\vartheta_0)$, when the compaction process is completed.

Aiming at a correct fitting approach, we presume the deformation ε to have no quantitative impact after the compaction has been completed.

Furthermore, we observe, that even under vanishing friction, the structure itself may effect a nonsymmetrical state, which lets the zero point have a value significantly less than unity.

Thus, we can formulate a convenient exponential fit with a high coefficient of regression and remaining well within the error margins:

$$k_a(\vartheta_0) = \alpha \exp(-\beta \vartheta_0).$$

Such an exponential approach implies the existence of a well defined value at the point of no friction and finally vanishing lateral stress in the limit of high angles of friction.

Drawn on a single logarithmic scale, the parameters are obtained easily from linear regression analysis (Fig. 16) as

$$\alpha = 0.62^{+0.10}_{-0.07}, \quad \beta = 0.036^{+0.0085}_{-0.0085}.$$

Furthermore, the exponential approach predicts $k_a(\mu_0 = 0) \simeq 0.62^{+0.10}_{-0.07}$, but due to its character as an extrapolation this value is very sensitive to variations of the parameters. Yet the value corresponds very well to the *"coefficient of redirection towards the wall"* for frictionless monodisperse granular media, $K \simeq 0.58$, cited by Duran [37].

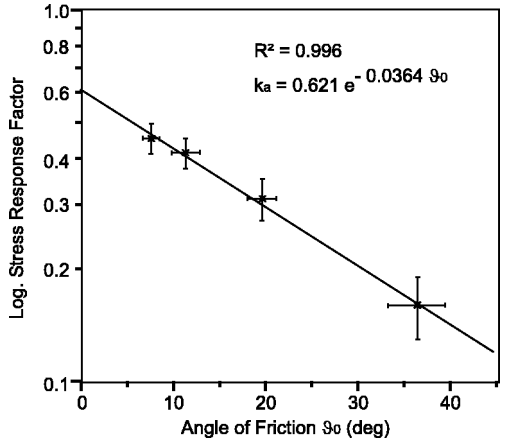

FIG. 16. Exponential fitting approach of lateral stress response (HLO).

VII. CONCLUSIONS

The results presented are, like all measurements, subject to appropriate interpretation, which can and need to be discussed further. However, concerning two-dimensional circular cylinders with diameters sharply distributed around a central value, they lead to the following conclusions.

Such granulate material, exposed to deformation of about 20% or more, can be well described using the model of Rankine or the later derivatives of it, as long as a structural correction has been applied to the coefficient of friction.

The structural correction contains terms of the distribution of diameters and the degree of deformation. Local irregularities of the surface do not play a significant role.

The dominant effect is the shifting of stable blocks against each other, where action takes place mainly in the shearing joint, allowing for a statistical approach.

If the deformation falls below this limit, reaching 10% to 5%, but is not zero, the behavior is dominated by effects of single cylinders, moving, rolling or gliding according to the local properties of contacts.

During this compaction process, local unevenness of the circumference of the cylinders is determined to be the most significant effect. Depending on the geometrical height and sharpness of irregularities, they substantially impede the compaction progress.

The measurements indicate that in a granular material consisting of smooth cylinders, even with varying frictional parameters, the compaction process is completed after unidirectional deformation of $\simeq 5\%$.

The resulting lateral stress response factor on compacted granular systems can be approximated as an exponentially decreasing function of the angle of friction.

ACKNOWLEDGMENTS

I wish to express my thanks to Dr. H.-J. Bösch, who largely supported this research work and to the Dr.-Ing. Leonard-Lorentz-Stiftung, who has made a major contribution to the experimental setup.

[1] H. M. Jaeger and S. R. Nagel, Science **255**, 1523 (1992).
[2] S. R. Nagel, Rev. Mod. Phys. **64**, 1523 (1992).
[3] B. Francoise, F. Lacombe, and H. J. Herrmann, Phys. Rev. E **65**, 031311 (2002).
[4] J. W. Rudnicki and J. R. Rice, J. Mech. Phys. Solids **23**, 371 (1975).
[5] D. M. Mueth, G. F. Debregeas, G. S. Karzmar, P. J. Eng, S. R. Nagel, and H. M. Jaeger, cond-mat/0003433.
[6] S. N. Coppersmith, C.-h. Liu, S. Majumdar, O. Narayan, and T. A. Witten, Phys. Rev. E **53**, 4673 (1996).
[7] C.-h. Liu, S. R. Nagel, D. A. Schecter, S. N. Coppersmith, S. Majumdar, O. Narayan, and T. A. Witten, Science **269**, 513 (1995).
[8] D. M. Mueth, H. M. Jaeger, and S. R. Nagel, Phys. Rev. E **57**, 3164 (1998).
[9] E. Bruce Pitman, Phys. Rev. E **57**, 3170 (1998).
[10] E. Bruce Pitman, Phys. Rev. E **57**, 3204 (1998).
[11] J. Duran, E. Kolb, and L. Vanel, Phys. Rev. E **58**, 805 (1998).
[12] D. Howell and R. P. Behringer, Phys. Rev. Lett. **82**, 5241 (1999).
[13] C. T. Veje, D. Howell, and R. P. Behringer, Phys. Rev. E **59**, 739 (1999).
[14] J. Astrom, H. J. Herrman, and J. Timonen, Phys. Rev. Lett. **84**, 638 (2000).
[15] S. Schollman, Phys. Rev. E **59**, 889 (1999).
[16] I. Jaky, Die klassische Erddrucktheorie mit besonderer Rücksicht auf die Stützwandbewegung, Abhandlung IVBH. Int. Ver. für Brückenbau und Hochbau I, 1938, Band 5.
[17] D. Mohr, Beiträge zur Theorie des Erddrucks, Zeitschrift des Architekten- und Ingenieurvereins zu Hannover, 1871/72, Hannover.
[18] G. Gudehus, in *Grundbau Taschenbuch 5. Auflage, Teil 1* (W. Ernst & Sohn, Berlin, 1996), p. 273 ff.
[19] G. Gudehus, Soils Found. **36**, 1 (1996).
[20] I. Herle, *Hypoplastizität und Granulometrie von Korngerüsten*. Publication No. 142 (Institute of Soil Mechanics and Rock Mechanics, University of Karlsruhe, Germany, 1997).
[21] D. Kolymbas, *Ein nichtlineares viskoplastisches Stoffgesetz für Böden*. Publication No. 77 (Institute of Soil Mechanics and Rock Mechanics, University of Karlsruhe, Germany, 1977).
[22] P. v. Soos, in *Grundbau Taschenbuch 5. Auflage, Teil 1* (Ref. [18]), p. 87 ff.
[23] W. Wu, *Hypoplastizität als mathematisches Modell zum mechanischen Verhalten granularer Stoffe*. Publication No. 129 (Institute of Soil Mechanics and Rock Mechanics, University of Karlsruhe, Germany, 1992).
[24] F. Radjai, D. E. Wolf, M. Jean, and J. J. Moreau, Phys. Rev. Lett. **80**, 61 (1998).
[25] Ch. A. Coulomb, Essai sur une application des règles de maximis es minimis à quelques problèmes de statique relatifs à l'architecture, —Mèmoires Acadèmie Royale des Sciences, Vol. VII, Annèe 1773-Paris, 1776.
[26] C. A. Coulomb, Acad. R. Sci. Mem. Phys. Diverse Savants **7**, 9 (1773).
[27] W. J. W. Rankine, Philos. Trans. R. Soc. London **147**, 9 (1857).
[28] W. J. M. Rankine, *Handbuch der Bauingenieurkunst nach der 12. Auflage deutsch bearbeitet von F. Kreuter* (Lehmann & Wentzel, Wien, 1880).
[29] O. Reynolds, Philos. Mag. **50**, 469 (1885).
[30] R. A. Bagnold, Proc. R. Soc. London, Ser. A **225**, 49 (1954).
[31] J. C. Geminard, W. Losert, and J. P. Gollub, Phys. Rev. E **59**, 739 (1999).
[32] P. A. Thompson and G. S. Grest, Phys. Rev. Lett. **67**, 1751 (1991).
[33] T. Pöschel and V. Buchholtz, Phys. Rev. Lett. **71**, 3963 (1993).
[34] J. R. Rice and A. L. Ruina, J. Appl. Mech. **105**, 343 (1983).
[35] T. Baumberger, P. Berthoud, and C. Caroli, Phys. Rev. B **60**, 3928 (1999).
[36] A. Gervois and D. Bideau, in *Disorder and Granular Media*, edited by D. Bideau and A. Hansen (North-Holland, Amsterdam, 1993).
[37] Jacques Duran, *Sands, Powders and Grains* (Springer-Verlag, New York, 2000).